Axonal precursor miRNAs hitchhike on endosomes and locally regulate the development of neural circuits

Eloina Corradi[1], Irene Dalla Costa[1*], Antoneta Gavoci[1*], Archana Iyer[1*], Michela Roccuzzo[1*], Tegan A. Otto[1], Eleonora Oliani[1], Simone Bridi[1], Stephanie Strohbuecker[1], Donatella Valdembri[3,4], Gabriela Santos-Rodriguez[2], Guido Serini[3,4], Cei Abreu-Goodger[2] and Marie-Laure Baudet[1]

1. Department of Cellular, Computational and Integrative Biology (CIBIO), University of Trento, via Sommarive 9, Povo 38123, Trento, Italy

2. Unidad de Genómica Avanzada (Langebio), Cinvestav, Irapuato 36824, Mexico

3. Candiolo Cancer Institute, FPO-IRCCS, 10060 Candiolo, Torino, Italy.

4. Department of Oncology, University of Torino School of Medicine, 10060 Candiolo
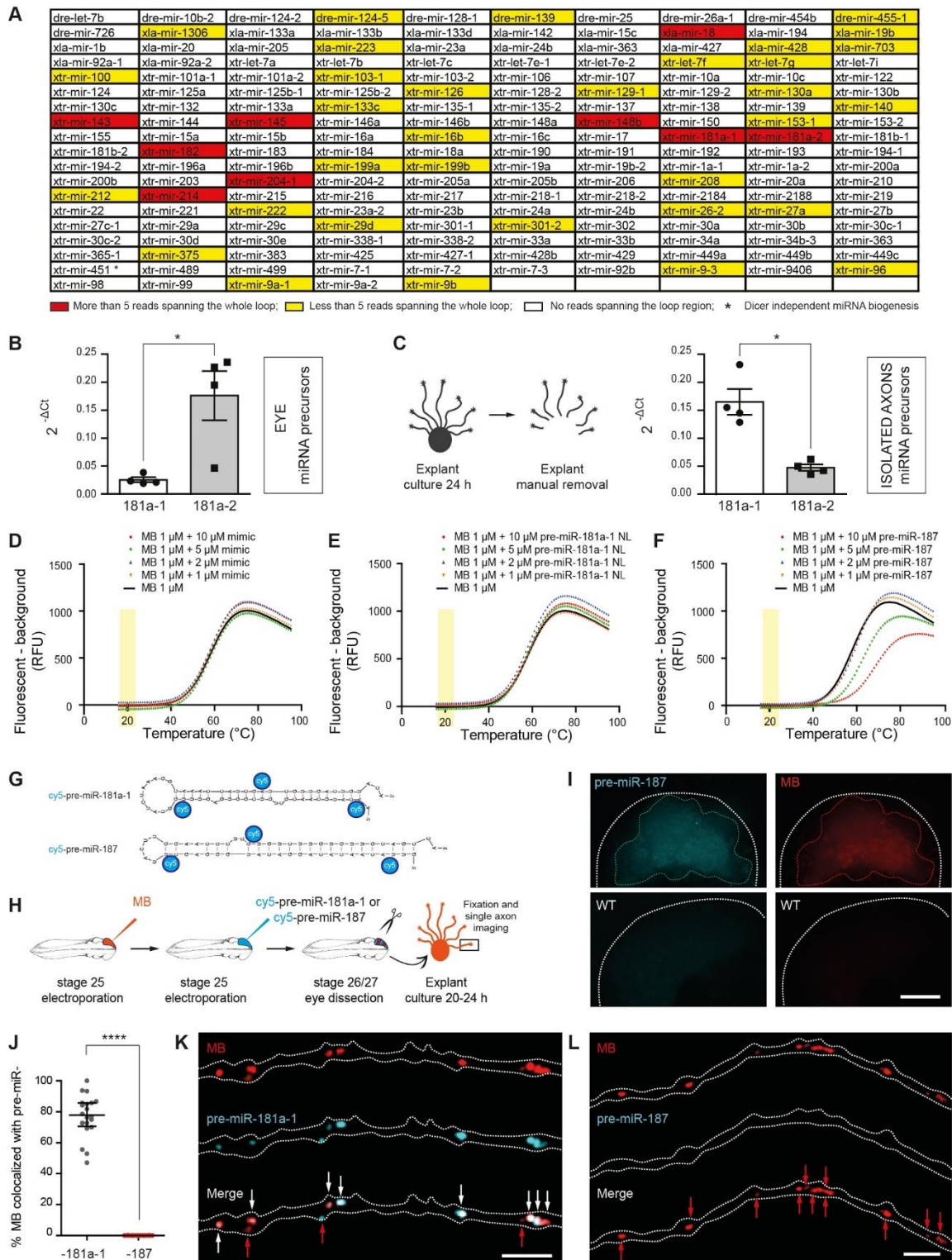
* Contributed equally

1) Appendix Figures

Appendix Figure S1.

Pre-miRNAs are present in RGCs axonal compartment

A. List of axonal miRNAs derived from (Bellon *et al*, 2017). Pre-miRNAs with more than 5 reads

mapping the hairpin loop were considered abundant.

B,C. Quantification of the expression levels of miR-181a-1- and miR-181a-2-precursors with the $2^{-\Delta Ct}$ method, using U6 as normalizer. Each data point represents one independent experiment. RNA was collected from 20 eyes or from isolated axons derived from 40 explants for each experiment. n=4 independent experiments. Values are mean ± SEM.

D-F. Thermal denaturation profiles of MB in the absence (solid black line) and presence (dashed line) of non-target miR-181-5p mimic (D), modified pre-miR-181a-1 without loop (E) and pre-miR-187 (F). Yellow boxes indicate the range of working temperatures for *ex vivo* trafficking experiments. Each melting curve represents the average of three independent experiments. Abbreviations: MB, molecular beacon; NL, modified pre-miR-181a-1 without loop.

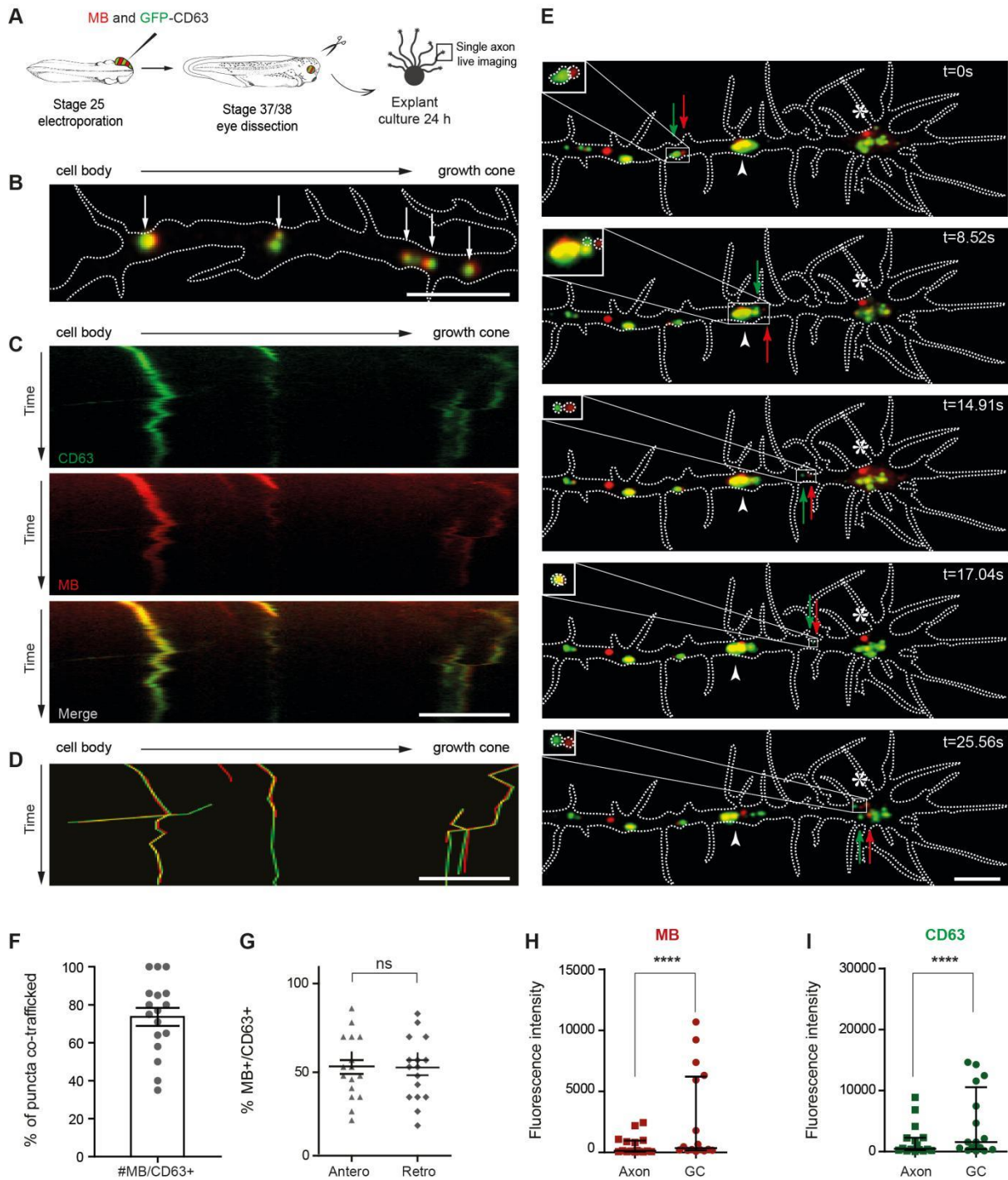G. Schematic representation of cy5-pre-miR-181a-1 and cy5-pre-miR-187.

H. Schematic representation of the experimental paradigm. Concentrations used: 5µM MB; 10ng/µL cy5-pre-miR-181a-1 or cy5-pre-miR-187. Abbreviations: MB, molecular beacon.

I. Representative image of electroporated (colored dashed lines, top panels) and WT (bottom panels) eye. The eye boundary is delineated with white dashed line. Abbreviations: WT, wild-type; MB, molecular beacon; pre-miR-187, cy5-pre-miR-187. Scale bars: 100µm.

J. Frequency (in percentage) of MB colocalizing with either cy5-pre-miR-181a-1 or cy5-pre-miR-187. Each data point represents one axon. Total number of puncta and axons analyzed: 601 puncta, 20 axons (MB/cy5-pre-miR-181a-1), 240 puncta, 19 axons (MB/cy5-pre-miR-187). n=3 independent experiments. Values are median with interquartile range. Abbreviations: MB, molecular beacon.

K,L. Representative images of electroporated axons. White and red arrows indicate, respectively, colocalized and non-colocalized MB puncta. Abbreviations: MB, molecular beacon; pre-miR-187, cy5-pre-miR-187. Scale bars: 5µm.

Data Information: * p<0.05, **** p<0.0001. Data were not normally distributed (Shapiro-Wilk test), two-tailed Mann Whitney test (B,C,J).

Appendix Figure S2.

Pre-miR-181a-1 trafficking is endosome mediated

A. Schematic of the experimental paradigm. Concentrations used: 5µM MB; 0.5µg/µL pCS2-CD63-eGFP. Abbreviations: MB, molecular beacon.

B. Snapshot of representative axon where MB-labeled pre-miR-181a-1 (red) and CD63-eGFP-labeled vesicles (green) are co-trafficked (white arrows). Scale bars: 5µm.

3

C. Representative kymographs generated from acquired time-lapse. Abbreviations: MB, molecular beacon; CD63, CD63-eGFP. Scale bars: 5μm.

D. Composite kymograph shown in (C) where the individual traces where drawn and color coded. Yellow trajectories represent MB-labeled pre-miR-181a-1 (red) and CD63-eGFP-labeled vesicles (green) co-trafficked. Scale bars: 5μm.

E. Representative time-lapse depicting MB-labeled pre-miR-181a-1 (red arrow) and CD63-eGFP-positive vesicles (green arrow) co-trafficked along the axon shaft to the growth cone (delineated with dashed white lines), wrist (white arrowhead) and central domain (white star). Abbreviations: MB, molecular beacon. Scale bars: 5μm.

F. Frequency (in percentage) of MB-labeled pre-miR-181a-1 co-trafficked with CD63-eGFP-positive vesicles. Each data point corresponds to one axon. Total number of puncta and axons analyzed: 174 puncta, 17 axons (MB+), 224 puncta, 17 axons (CD63+). n=5 independent experiments. Values are mean ± SEM. Abbreviations: MB, molecular beacon; CD63, CD63-eGFP; GC, growth cones.

G. Frequency distribution (in percentage) of MB-labeled pre-miR-181a-1 co-trafficked with CD63-eGFP-positive vesicles. Each data point corresponds to one axon. Total number of puncta and axons analyzed: 57 puncta, 17 axons (anterograde), 59 puncta, 17 axons (retrograde). n=5 independent experiments. Values are mean ± SEM. Abbreviations: ns, not significant; MB, molecular beacon; CD63, CD63-eGFP.

H,I. Fluorescence intensity of MB (H) and CD63 (I) measured in axon and the growth cone central domain. Each data point corresponds to one axon or a growth cone central domain. Total number of axons analyzed: 16. n=5 independent experiments. Values are median with interquartile range. Abbreviations: MB, molecular beacon; CD63, CD63-eGFP.

Data information: *** $p < 0.001$, **** $p < 0.0001$ Data were normally distributed (Shapiro-Wilk test). Unpaired t-test (G). Data were not normally distributed (Shapiro-Wilk test). Wilcoxon matched-pair test (H,I).
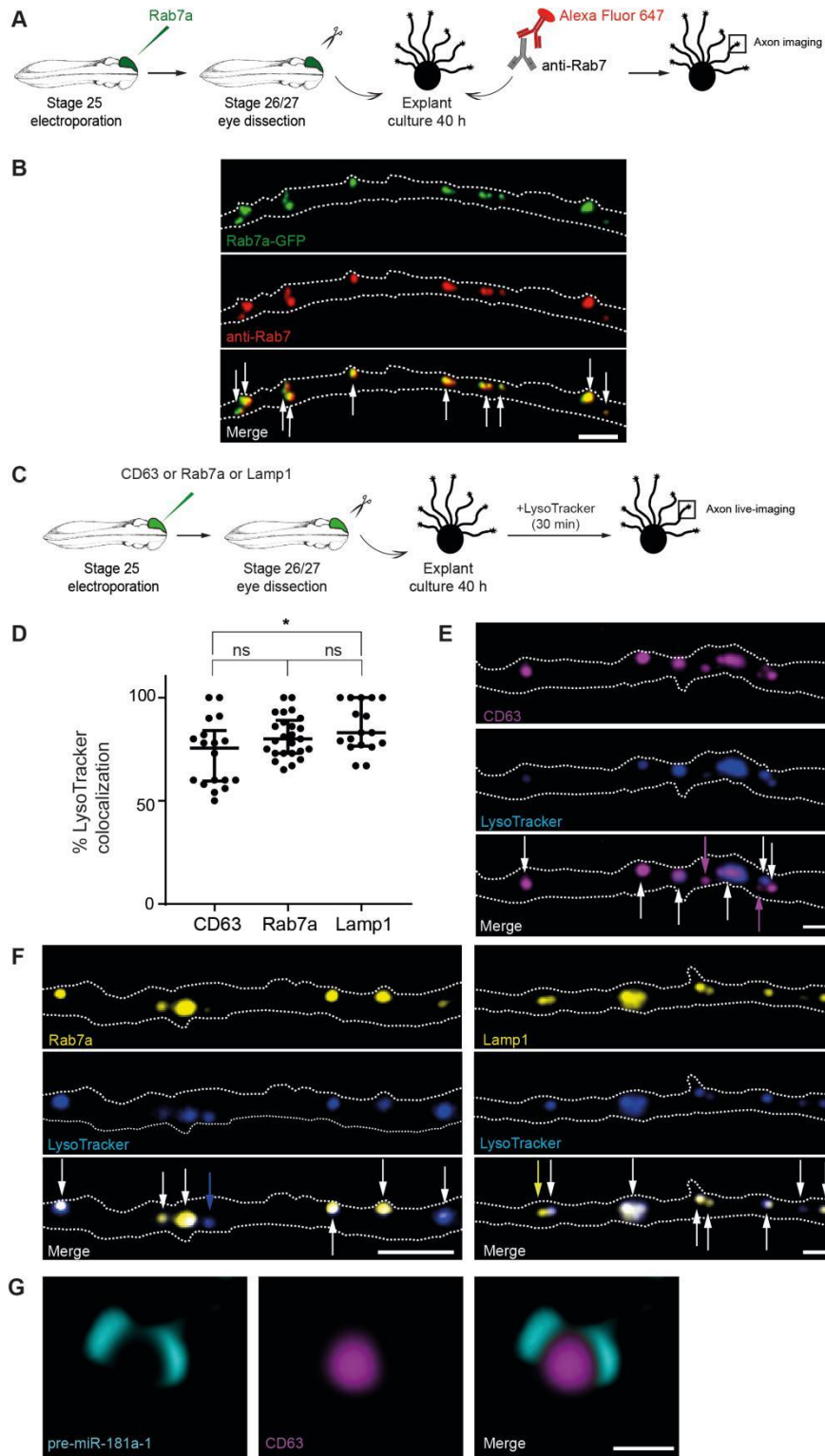
Appendix Figure S3.

Rab7a-GFP matches endogenous Rab7a expression and LysoTracker is highly colocalized with late endosome / lysosome markers.

A. Schematic representation of the experimental paradigm. Plasmid concentrations used: 0.4µg/µL pCS2-Rab7a-eGFP; 0.5 µg/µL of pCS2-Rab7a-mRFP. Abbreviations: Rab7a, Rab7a-eGFP or Rab7a-mRFP.

B. Representative image of colocalization of Rab7a with anti-Rab7 antibody. 100% colocalization was observed. Dashed white line delineates the axon. White arrows represent colocalized puncta. Each data point represents one axon. Total number of puncta and axons analyzed: 253 puncta, 12 axons. n=2 independent experiments. Abbreviations: Rab7a, Rab7a-eGFP or Rab7a-mRFP. Scale bars: 5µm.

C. Schematic representation of the experimental paradigm. Plasmid concentrations used: 0.5µg/µL pCS2-CD63-eGFP or pCS2-Lamp1-eGFP; 0.4µg/µL pCS2-Rab7a-eGFP; 50nM LysoTracker. Abbreviations: CD63, CD63-eGFP; Rab7a, Rab7a-eGFP or Rab7a-mRFP; Lamp1, Lamp1-eGFP.

D. Frequency (in percentage) of signal colocalization between LysoTracker and CD63, Rab7a or Lamp1. Each data point corresponds to one axon. Total number of puncta, axons and independent experiments analyzed: 416 puncta, 18 axons, n=3 (LysoTracker/CD63), 729 analyzed puncta, 25 axons, n=2 (LysoTracker/Rab7a), 638 analyzed puncta, 17 axons, n=2 (LysoTracker/Lamp1). Values are median with interquartile range. Abbreviations: CD63, CD63-eGFP; Rab7a, Rab7a-eGFP or Rab7a-mRFP; Lamp1, Lamp1-eGFP; ns, not significant.

E,F. Representative images of colocalization between LysoTracker and CD63 (E), Rab7a or Lamp1 (F). Dashed white line delineates the axon. White arrows represent colocalized puncta; magenta, yellow and blue arrows represent not colocalized puncta for CD63 (E), Lamp1 (F) and LysoTracker (F), respectively. Abbreviations: CD63, CD63-eGFP; Rab7a, Rab7a-eGFP or Rab7a-mRFP; Lamp1, Lamp1-eGFP. Scale bars: 5µm.

G. Representative 3D-STED super-resolution image. Total number of puncta, axons and growth cones analyzed: 99 puncta, 16 axons and 10 growth cones (MB), 291 puncta, 36 axons and 15 growth cones (cy3-pre-miR-181a-1). n=2 (MB), n=3 (cy3-pre-miR-181a-1) independent experiments. Abbreviations: pre-miR-181a-1, cy3-pre-miR-181a-1; CD63, CD63-eGFP. Scale bars: 200nm.

Data information: * p<0.05. Data were not normally distributed (Shapiro-Wilk test). Kruskal-Wallis test

followed by Dunn's multiple comparison *post hoc* test (D).
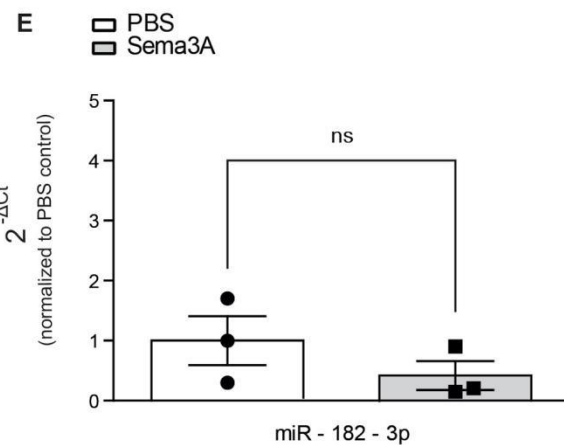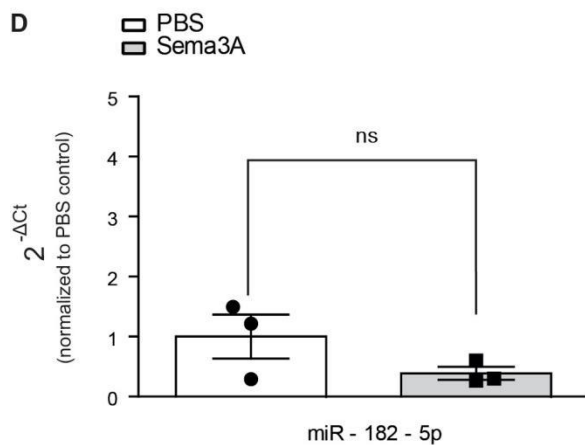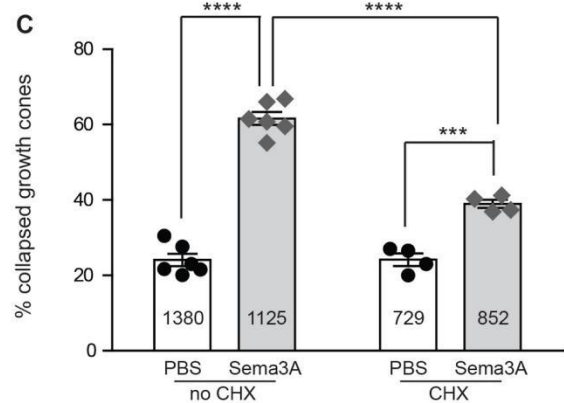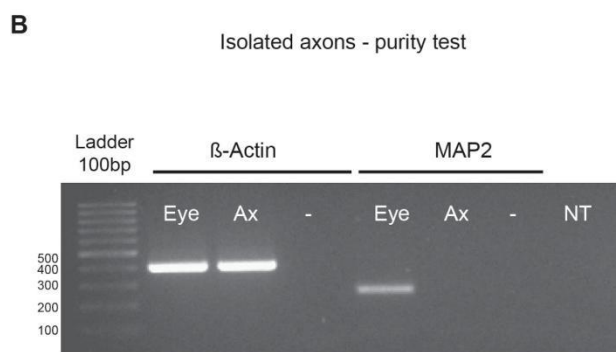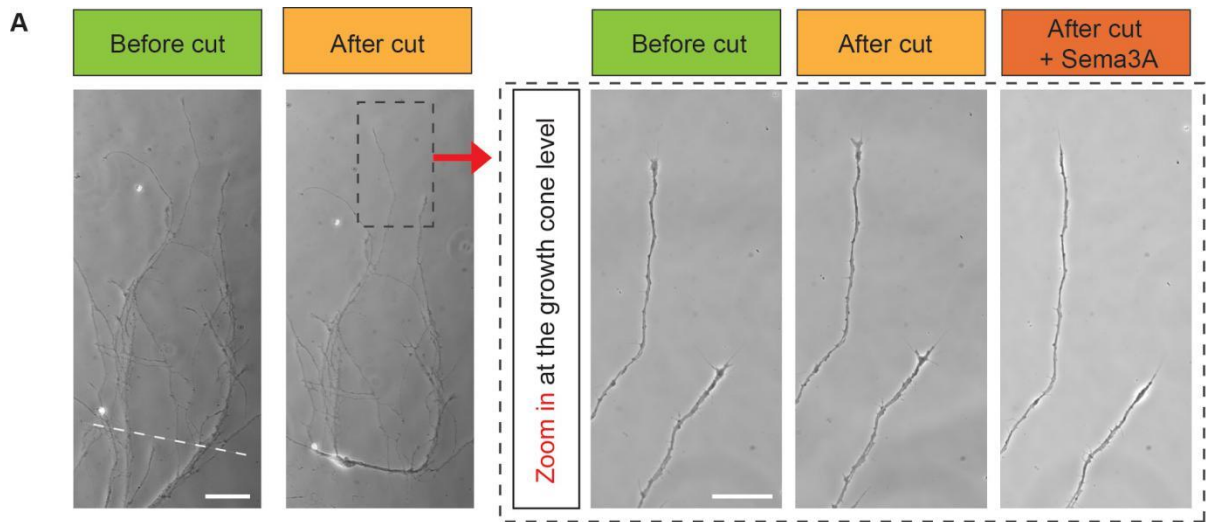
Appendix Figure S4.

Validation of axonal sample preparation and translation- dependent cue-induced collapse

A. Representative image of stage 37/38 RGC axons cultured for 24 h, before and after explant removal. Zoom-in panels illustrate that growth cones still adopt a stereotypical shape after removing the explant ("cut") suggesting that axonal health is maintained; axons also stay responsive to cues as demonstrated by Sema3A-induced collapse. Scale bars: 50μm (A, left), 30μm (A, right).

B. RT-PCR from RNA extracted from isolated axons or from stage 37/38 whole eyes. β-Actin mRNA is present both in eye and axon, while MAP2 mRNA is present only in eye, suggesting absence of dendritic material in the axonal samples. Abbreviations: Ax, isolated axon; NT, no template RT negative control; -, no template PCR negative control.

C. Frequency (in percentage) of collapsed growth cones from stage 37/38 embryos, following a 10 min Sema3A bath application. Concentrations used: 200ng/mL Sema3A; 50μM cycloheximide (CHX). CHX was applied to block translation. Total number of counted growth cones is reported in the column. Each data point corresponds to one independent experiment. n=3 independent experiments. Values are mean ± SEM. Abbreviations: CHX, cycloheximide.

D,E. Quantification of miR-182-5p (D) and miR-182-3p (E) expression levels using the $2^{-\Delta Ct}$ method and U6 as normalizer, upon Sema3A stimulation. Data are normalized to PBS control. Each data point represents one independent experiment. n=3 independent experiments. Values are mean ± SEM. Abbreviations: ns, not significant.

Data information: *** $p < 0.001$, $p < 0.0001$ Data were normally distributed (Shapiro-Wilk test). Two-way ANOVA followed by Tukey's multiple comparison *post hoc* test (C). Unpaired t-test (D,E).
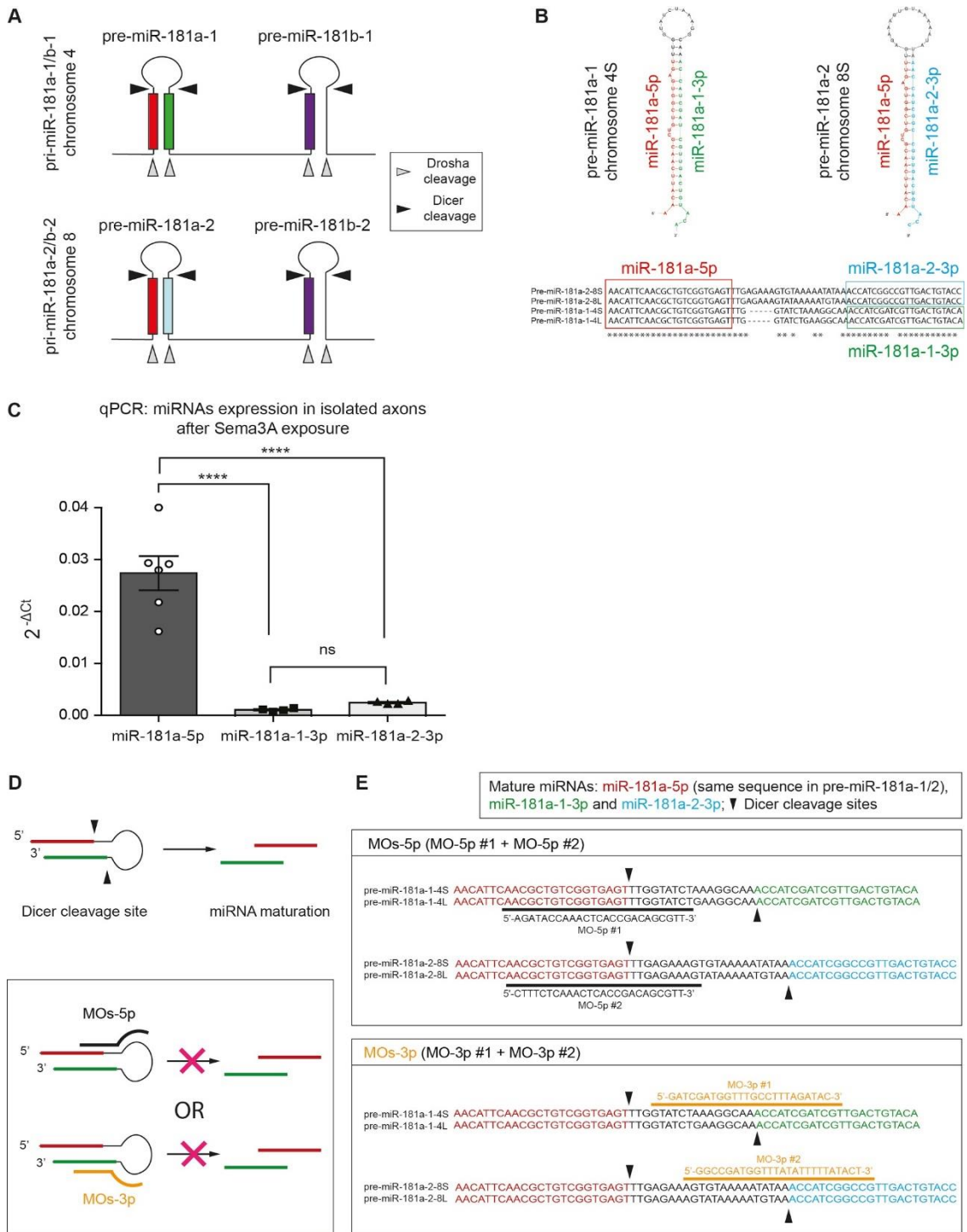
Appendix Figure S5.

Pre-miR-181a-1/a-2 schematics

A. Schematic representation of pri-miR-181a-1/b-1 on chromosome 4 and of -181a-2/b-2 on chromosome 8. Small gray and black arrowheads indicate Drosha cleavage sites and the black ones Dicer cleavage sites, respectively. Colored boxes show the position of mature miRNAs.

B. Predicted secondary structure (Mfold v3.6) and multiple alignment (MUSCLE v3.8) of the two precursors isoforms, pre-miR-181a-1 (chromosome 4S) and pre-miR-181a-2 (chromosome 8S).

C. Quantification of the expression levels of miRNAs using the $2^{-\Delta Ct}$ method and U6 as normalizer. miR-181-5p was 24.30 and 10.11 fold higher than miR-181-1-3p and -2-3p, respectively. RNA was collected from stage 40 isolated axons for each experiment. Each data point represents a single RT-qPCR reaction. n=3 (miR-181-3p), n=4 (miR-181-1-5p) independent experiments. Values are mean ± SEM. Abbreviations: ns, not significant.

D. Schematic of pre-miRNA maturation upon Dicer cleavage (top panel). Schematic of MOs-5p and MOs-3p targeting 5' and 3' pre-miRNA Dicer cleavage site respectively (bottom panel).

E. Exact MO targeting region within pre-miR-181a-1 and -2 derived from chromosomes 8, and 4, long (L) or short (S). Black arrowheads indicate Dicer cleavage sites.

Data information: *** $p<0.001$, **** $p<0.0001$. Data were normally distributed (Shapiro-Wilk test). One-way ANOVA followed by Tukey's multiple comparison *post hoc* test (C).
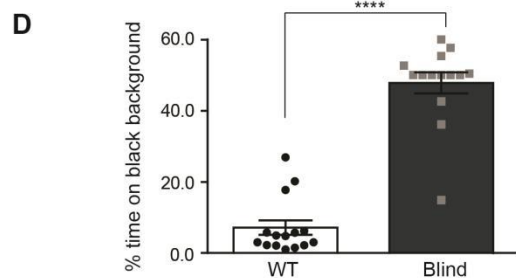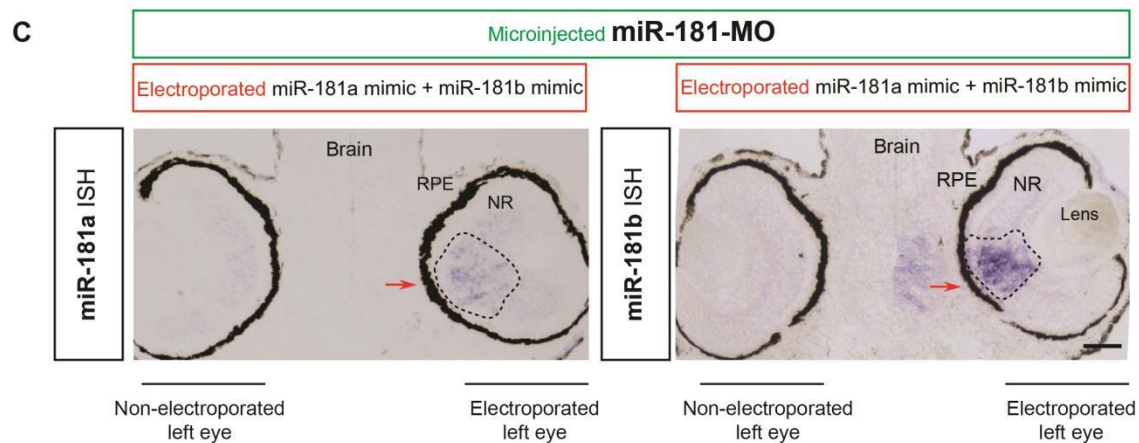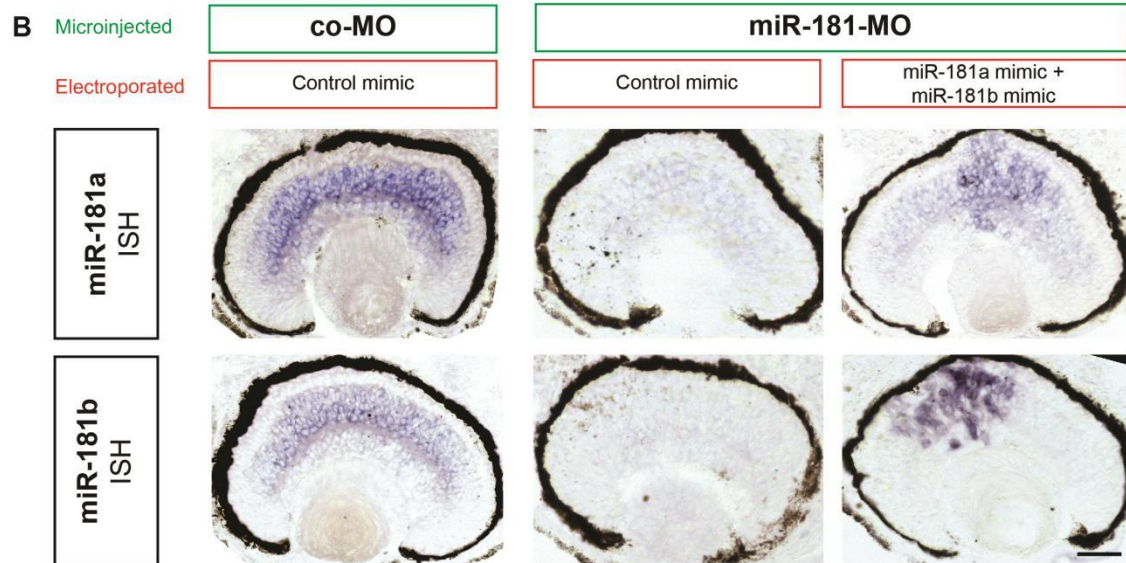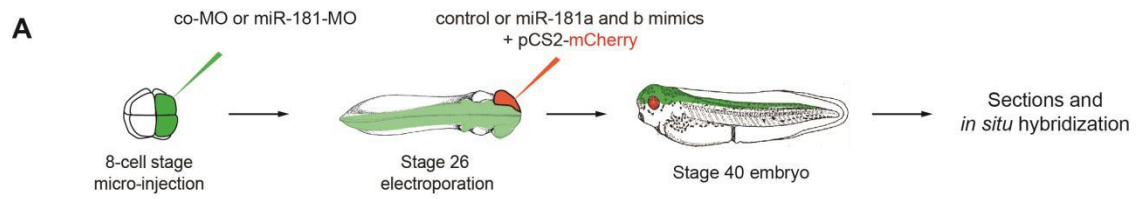
Appendix Figure S6.

Mimics rescue miR-181 loss of expression

A. Schematic representation of the experimental paradigm. Microinjection mixture concentrations:

pre-miR-181a-1-, pre-miR-181a-2- and miR-181b-MO at 0.4ng each in 1nL (miR-181-MO); custom

control plus standard control MOs (co-MO) at 0.6ng each in 1nL. Electroporation mixture concentration: 0.5μg/μL pCS2-mCherry; 50μM miRNA mimic cocktail (25μM miR-181a-mimic + 25μM miR-181b-mimics or 50μM control mimics). Abbreviations: 3'CF, 3'Carboxyfluorescein; co-MO, control morpholino; miR-181-MO, morpholino targeting mix.

B. ISH on cryosections using miR-181a and b specific LNA probes. miR-181a and b are distributed in the inner nuclear and ganglion cell layer. Note the absence of signal upon miR-181 loss-of-function and how this signal is rescued specifically in areas electroporated with miR-181a and b mimics. Abbreviations: co-MO, control morpholino; miR-181-MO, morpholino targeting mix. Scale bars: 50μm.

C. ISH on cryosections as in (B) where brain and contralateral eye to the electroporated retina are also visible. Note the absence of miR-181 signal in both right and left retina except in the electroporated region (red arrow, delineated with dashed black lines). Abbreviations: miR-181-MO, morpholino targeting mix; RPE, retinal pigment epithelium; NR, neural retina. Scale bars: 50μm.

D. Frequency distribution (in percentage) of the amount of time embryos spent on average on black background. "Blind" indicates eyeless embryos. Numbers on the columns are the total number of embryos analyzed. Each data point represents one embryo. Total number of embryos analyzed: 15 (WT), 14 (Blind). Values are mean ± SEM. Abbreviations: WT, wild-type.

Data Information: **** $p < 0.0001$ Data were not normally distributed (Shapiro-Wilk test). Two-tailed Mann Whitney test, 4 independent experiments (D).

MATERIAL AND METHODS - APPENDIX

In vitro **MB thermodynamics**

The thermodynamic characteristics of the MB was assessed by thermal denaturation profile in which the fluorescence signal was recorded as a function of temperature, both in the absence and presence of the target (pre-miR-181a-1) or non-target (pre-miR-187, miR-181a-5p mimic, modified pre-miR-181a-1 without the loop region [see Table EV4 for sequence]) sequences. The thermocycler program used was 15°C for 3 min, then from 16°C to 95°C increasing 1°C/min. Denaturation profiles confirmed the suitable thermodynamic characteristics of our MB design: low fluorescence at low temperature and a melting temperature (Tm) of 58°C, appropriate for our working temperature of 20°C (Simon *et al*, 2010; Søe *et al*, 2011).

Immunohistochemistry on mice

P0 brains and E13.5 whole heads were fixed in 4% PFA (Life Technologies) overnight, washed and transferred into 30% sucrose (ACS reagent) at 4°C until sunk. Samples were embedded in OCT (Leica) and 14 µm sections were obtained with Leica CM 1850 UV cryostat.

Antigen retrieval was performed in a steamer for 25 min by immersion in pH6 10 mM sodium citrate (Sigma). Sections were permeabilized in 0.1% Triton X-100 (Fisher Chemical) and blocked with 10% heat inactivated goat serum (HIGS, Gibco) for 2 hours at room temperature. Rabbit anti-HA Y-11 (sc-805, 1:50, Santa Cruz Biotechnology) was used to stain Dicer-HA, mice anti-neurofilament (3A10, 1:500, DSHB) was used to track neurons. Primary antibodies were incubated overnight at 4°C. Secondary antibodies Alexa 488 anti-rabbit or 594 anti-mouse (Life Technologies) were used at 1:1000 and incubated 1 hour at room temperature. Sections were counterstained with nuclear marker ToPro (T3605, 1:1000, Molecular probes) and mounted with Prolong Gold (Invitrogen).

Slides were acquired with confocal Leica TCS SP5 microscope or confocal Leica SP8 with white light lasers using a 40x objective. A zoom factor of 3 (Fig 5C and Fig EV2C) or 1.99 (Fig 5D) was applied during acquisition and a Z-stack of 6-14µm depth applied in order to capture the axons projections

(Fig 5D). Gain and offset were optimized for best signal to noise ratio and the settings were maintained throughout acquisitions.

In situ hybridization

DIG-labeled LNA oligonucleotides complementary to *Xenopus laevis* miR-181a , xtr-miR-181b and scrambled probes (Table EV4) were obtained from Exiqon and added at 1nM. 14µm sections containing eye and brain of fixed stage 40 embryos were obtained using a Leica CM1850 UV cryostat, collected on SuperFrost slides (Thermo Scientific) and processed for ISH as described previously (Baudet *et al*, 2012). Acetylation was carried out for 10 minutes in 442 mL of DEPC water, 952µL HCl (Sigma), 6mL triethanolamine (Sigma) and 1.25mL of acetic anhydride (Sigma). 5µg/mL Proteinase K (Euroclone) was applied for 5 minutes. The pre-hybridization step was performed at room temperature for 4 hours, followed by incubation of the hybridization solution containing denatured probe for 16 hours at 55°C. Sections were washed with 5x and 0.2x SSC (Gibco) at 55°C, blocked with 10% sheep serum (Jackson) at room temperature for 1 hr and stained with anti-digoxygenin antibody (Immunoresearch, 1:2000) incubated overnight at 4°C. Slides were then imaged on upright widefield Zeiss Imager M2 fluorescence microscope equipped with AxioCam MRc color camera 5 Megapixel, using EC Plan Neofluar 20X/0.5 and 10X/0.3 objectives.

Blastomere Microinjection

Morpholino mixtures were injected into both dorsal animal blastomeres of eight-cell-stage embryos after jelly coat removal, placing the embryos into an injection dish containing 4% Ficoll (Carl RothGmBH) and using a 1.0mm outer diameter (OD) x 0.5mm internal diameter (ID) glass capillary injection needle (Harvard Apparatus). The concentration and mixture used in each experiment are specified in the figure legends.

MO used for electroporation

The concentration and mixture used in each experiment are specified in the figure legends. For miR-181-MO cocktail, a 250µM morpholino mixture of 62.5µM pre-miR-181a-1-MO, 62.5µM pre-miR-

181a-2-MO and 125µM miR-181b-MO was used, and matched with a control MO cocktail (co-MO; 125µM custom control plus 125µM standard control) (Fig 7). This miR-181 MO cocktail was used to block the processing of pre-miR-181a-1 and pre-miR-181a-2 and thus the function of miR-181a-5p, -1-3p and -2-3p. Since miR-181a-5p and miR-181b share the same seed and differ by only 4 nucleotides, we also used a MO to block miR-181b function to avoid any functional redundancy. In order to rescue miR-181 isoforms KD upon miR-181-MO cocktail, a mix of miR-181 mimics were used (25µM miR-181a-, plus 25µM miR-181b-mimic), matched with 50µM control mimics (Fig 7). See Table EV4 for exact sequences.

MO used for axon co-transfection

The MO mix used in the co-transfection performed in Fig 9G was constituted by a total morpholino concentration of 4 µM. In the MOs-3p + MOs-TUBB3 condition the mix was formed by 1µM MO-3p #1 + 1µM MO-3p #2 + 1µM MO TUBB3 L + 1µM MO TUBB3 S. In the MOs-3p + co-MO condition the mix was formed by 1µM MO-3p #1 + 1µM MO-3p #2 + 2µM of control MO (co-MO, standard control). In the co-MO condition the mix was formed by 4µM of control MO (co-MO, standard control). See Table EV4 for exact sequences.

Open book preparation

Stage 40 or 44/45 fixed embryos were secured on a sylgard plate, brains were dissected and cut on the ventral midline to open the two hemispheres. Open brains were placed on a 24mm circular glass coverslip (Marienfeld) inside two reinforcement labels of 12mm (Niji), closing the prepared sample with a 12mm glass coverslip (Marienfeld) on top. Brains were acquired using a Leica DMi8 inverted fluorescence microscope. The z-stacks of serial images comprising the entire contralateral optic pathway were captured. Bright-field images were acquired as a reference of the tectum position. Axons were considered as straying when they abnormally looped, twisted or bent within the tectum.

Behavioral assay

Embryos were grown until stage 44/45 on a white background in 12 h light/12 h dark environment. The behavioral assay was performed according to (Viczian & Zuber, 2014) with minor modifications. Embryos were grown in home made tanks whose walls were partitioned into black and white. A webcam (Logitech) was fixed to image the whole tank. One embryo at a time was gently released into the top black corner of a partitioned black/white tank and recorded for 2 min. Then, the black and white bottom of the tank was turned, and the embryo's movements recorded again. This was repeated 6 to 8 times per embryo. The amount of time each embryo stayed on the black side was measured and expressed as a percentage of the whole movie's duration (at least 120 s).

***Xenopus* RGC dissociated cells**

Stage 37/38 electroporated eyes were dissected and washed twice in 60% L-15 and 1% Antibiotic-Antimycotic (ThermoFisher). Eyes were then transferred to 100 μL Trypsin-EDTA 0.25% (ThermoFisher, kind gift from Marina Mione), incubated for 2 min, and thoroughly mixed by pipetting. Trypsin reaction was blocked by adding 900 μL of 0.9X PBS + 10% FBS + Penicillin-Streptomycin (Gibco, kind gifts from Marina Mione). After 3 min of centrifugation at 900 rpm, the supernatant was discarded and the pellet was resuspended in 200μL of 60% L-15 and 1% Antibiotic-Antimycotic (ThermoFisher) and cultured at 20°C for 20-24h at ~ 94 cells/mm^2. RGCs were identified through the phase by its stereotypical shape.

Acquisitions were performed with an inverted Leica DMi8 epifluorescence microscope equipped with a sCMOS monochromatic camera (AndorZyla 4.2 Megapixel) and with a HC PL ApoCS2 63x/1.4 oil objective. The acquisition mode was set to 12-bit grayscale, "low noise"and "high well capacity". Exposure time was kept as low as possible for all channels (100ms).

Culture and *Xenopus* embryos fixation

Cultures were fixed in 2% PFA (Life Technologies), 7.5% sucrose (ACS reagent) for 30 min. Embryos were fixed in 4% PFA for 2 hours at room temperature then rinsed three times in 1X PBS (Gibco).

Laser capture microdissection (LCM) *ex vivo*

Stage 37/38 retinal cultures on RNase free Polyester membranes (Leica) were stained with FM-1-43FX dye (Thermo Fisher) for 20 min, fixed in 1% PFA (Life Technologies) for 5 min and dehydrated in ethanol (Sigma) 25%, 50%, 75%, 90% and 100%) for 1 minute each. Axons were captured using the Leica microdissector LMD6500 with the following settings: 20X and 40X (magnification), 33-38 (power), 1 (aperture), 16-14 (speed), 0 (specimen balance), 50 (offset).

Immunohistochemistry on *Xenopus*

Fixed explants were permeabilized with 0.1% Triton X-100 (Fisher Chemical) and blocked with 5% HIGS (Gibco) for 1 hour. Mouse monoclonal anti-Ago2 (a kind gift from Dónal O'Carroll, 1:50), rabbit anti-Dicer (sc-30226, 1:50, Santa Cruz Biotechnology) and rabbit anti-Rab7 (137029 ,1:2000, Abcam) were used. Primary antibodies were diluted in 5% HIGS (Gibco) incubated overnight at 4°C. Secondary antibodies Alexa Fluor AF-488 anti-mouse (1:1000), AF-594 anti-rabbit (1:1000) or AF-647 (1:2000, Life Technologies) were incubated 1 hour at room temperature. Explants were mounted either with Prolong Gold (Invitrogen) (Fig 5B) or Prolong Diamond (Invitrogen) (Appendix Fig S3B).

Zeiss observer Z1 microscope equipped with AxioCam MR3, 1.4 Megapixel camera or Leica Dmi8 microscope coupled with AndorZyla 4.2 Megapixel camera, were used with a HC Plan Apochromat CS2 63X/1.4 Oil objective.

g-STED confocal scanning microscopy

To acquire super-resolved images, a Leica TCS SP8 gated-stimulated emission depletion (g-STED) 3X laser-scanning microscope equipped with a HC PL APO 100X/1.40 objective was employed (Leica Microsystems). Fluorochromes were excited at the optimal wavelength by means of 80 MHz pulsed white light laser (470–670 nm), allowing time gating of fluorescence life times. For STED, the appropriate, 592 or 660 nm, depletion laser was used. Fluorescence channels were scanned sequentially and emission was revealed by means of hybrid spectral detectors (HyD SP Leica

Microsystems). STED images were deconvolved to reduce noise using the mathematical algorithm Classic Maximum Likelihood Estimation (CMLE) included in Huygens Deconvolution Software.

MSD analysis

Region of interest containing a segment from a single axon but not its growth cone was selected. Trajectories of single cy3-particles were recovered with Fiji/ImageJ using TrackMate plugin for automated single-particle tracking (Tinevez *et al*, 2017). To discriminate trajectories of particle that underwent directed motion from nonspecific noise and immobile objects, we selected trajectories based on their total displacement (minimum of 2.9 µm) and duration (80 consecutive frames). For each recovered trajectory, the mean square displacement (MSD) was calculated as follows: $MSD(\tau) = \langle(x(t+\tau)-x(t))^2+(y(t+\tau)-y(t))^2\rangle$ (Eq2) where x and y are the coordinates of the particle along the axon, t and τ are the absolute and lag times, respectively, and the brackets represent the time average. This calculation was performed for τ=25% of the total time of the trajectory (Ruthardt *et al*, 2011).

The MSD data were fitted with an anomalous diffusion model: $MSD=A\tau^\alpha+B$ (Eq1) where A depends on the motion properties of the particle, B is the residual MSD, and the coefficient α is an indication of the particle motion-type (Otero *et al*, 2014). Trajectories were classified as actively driven ($\alpha>1.5$), diffusive ($0.9<\alpha<1.1$) or confined ($\alpha<0.5$). Diffusion D was calculated for those particles moved only by diffusion according to $D=MSD/qt$ (Eq3) where t is time and q is a constant depending on the dimension of the fitting model (q=2Xdim=4 in our case). Eq1 can be rewritten as $t=r^2/4D$ (Eq4) where t is time in seconds, and r is the displacement length in µm. We considered that the distance from *Xenopus laevis* RGC cell bodies to the tip of axons is 500µm (Turner-Bridger *et al*, 2018).

RNA extraction

Single Cell RNA Purification Kit (Norgen) was used to extract total RNA from axonal samples following the manufacturer's instructions. In the lysis step, 200µL of the lysis buffer (Buffer RL, Norgen) were

mixed with β-mercaptoethanol (Sigma, 1:100), added to the axonal culture and incubated for 5 minutes. RNA was eluted by applying 9μL Elution Solution twice to the column. Total RNA from eyes was extracted using Norgen Total RNA Purification Micro Kit (Norgen) following the manufacturer's instructions and running an on-column RNAse free-DNAse I treatment (Norgen). For small fraction RNA collection the Split kit (Lexogen) was used, following the manufacturer's instructions. The integrity and concentration of RNA obtained from isolated axon samples was assessed using the Agilent RNA 6000 Pico kit (Agilent technologies, Germany) on a Bioanalyzer (Agilent 2100 Bioanalyzer, Germany) for sensitive applications from small sample size (LCM & RNA-seq).

RNA retrotranscription

3-5 μL axonal RNA, or 10 ng total RNA from eye samples were retrotranscribed with SuperScript® IV (Thermofisher) using random hexamers primers (Euroclone) following the manufacturer's instructions. miRNA retrotranscription was performed with TaqMan™ MicroRNA Reverse Transcription Kit (Thermofisher) and the TaqMan qPCR assay (Thermofisher) following the manufacturer's instructions.

PCR and gel visualization

2μL 1:3 diluted cDNA (from isolated axon preparation), or 3-4μL undiluted cDNA (from LCM axonal collection) were used as input for GoTaq G2HotStart Polymerase (Promega) PCR reaction following the manufacturer's instructions. For mice genotyping, a small piece of tail was collected post-mortem, DNA was extracted by alkaline lysis incubating the sample in 50mM NaOH (Sigma) for 1 hour 95°C 400 rpm, followed by neutralization with 1M Tris-HCl (pH 8) and centrifuged at 5000 rpm for 10 min. 4μL of the supernatant were used directly as input for the PCR reaction. PCR products were loaded on a 2% TAE (Euroclone) or 3% TBE (Thermofisher) agarose gel (Sigma Aldrich), run at 5.5V/cm on an electrophoretic apparatus (BioRad) and visualized with UVITec Alliance LD2. The DNA was stained with Clear Sight DNA Stain (Bioatlas). Primers list in Table EV4.

Identification of axonal RNA for miR-181 target prediction

10 ng of axonal RNA collected from isolated axons and purified with SPRI beads (Beckman Coulter) was used as input for the Ovation SoLo RNA-Seq System, Custom AnyDeplete (NuGEN) and sequenced using NextSeq 500-MID, paired-end 80 nt approach (Illumina) at the EMBL Genomics Core facility (Heidelberg, Germany). Using the AnyDeplete system, *Xenopus laevis* rRNA sequences identified through the NCBI nucleotide and the SILVA databases (Quast *et al*, 2012) were removed.

After ensuring raw sequence read quality with FastQC, reads were trimmed using Trimmomatic according to the Ovation SoLo RNA-Seq System instructions. Additionally, we removed adapter sequences and reads shorter than 40 bp. Trimmed reads were mapped with HISAT2 (Bolger *et al*, 2014), using default settings apart from --rna-strandness FR, to the *Xenopus* laevis genome (9.1) with an added rRNA contig and subsequently sorted using samtools (Li *et al*, 2009).

Using the *Xenopus laevis* transcriptome annotation (v.1.8.3.2 from xenbase.org), reads mapping to genes were quantified with FeatureCounts (Liao *et al*, 2014) using the following parameters: -p -t exon -g gene_id -s 1. The expression levels for each gene were calculated using the rpkm() function from the edgeR package (Robinson *et al*, 2010). We identified genes as axonally present if they were detectable at or above 1 FPKM.

Live imaging of pre-miR trafficking acquisition settings

Live imaging was performed using an inverted Leica Dmi8 epifluorescence microscope equipped with a sCMOS monochromatic camera (AndorZyla 4.2 Megapixel) and with a HC PL ApoCS2 63x/1.4 oil objective (Fig 3B-E and Appendix Fig S2B-E and Movies EV1-3 and EV5) . The acquisition mode was set to 12-bit grayscale, "low noise", "no binning", and "high well capacity". Live imaging upon Vincristine (Alexis Biochemicals, kind gift from HTS facility, CIBIO) drug application was performed using an inverted Nikon Ti2 equipped with the X-light X2 spinning disc, a sCMOS monochromatic camera (AndorZyla 4.2 Megapixel) and a plan Apochromatic 60x/1.4 oil objective. The acquisition mode was set to 12-bit and Gain 4 with a "Readout Rate" of 540 MHz, no binning, "Rolling Shutter" as Readout

Mode and overlap as "Sensor Mode". Time-lapse for cy3-pre-miR-181a-1 (Eurofins Genomics) consisted of 400 frames with "no delay" mode applied (Movie EV4). No binning was applied to any acquisition. Exposure time and light intensity were chosen to optimize the signal to noise ratio, but were always kept invariant for the same batch of analysis. Exposure time was kept as low as possible (100-150 ms).

Pre-miRNA and CD63 fluorescence quantification in axons and growth cones

For digital quantitation, pixel saturation was strictly avoided and the mean pixel intensity of CD63 and MB fluorescence was measured from the first frame of the live imaging acquisition. To define the area for digital fluorescence quantification, the outline of the central domain of each growth cone and their corresponding axon (70 µm from the growth cone wrist) were manually traced. ImageJ software was used to calculate the mean pixel intensity per unit area. Each trace was then superimposed in an area devoid of biological material, located immediately adjacent to the axon/central domain of the growth cone to record the background fluorescence. This reading was then subtracted from the CD63/MB reading. The background-corrected intensities of each areas were plotted and differences were analyzed for statistical significance, pairing growth cone and axon of the same neuron. Only single axons were analyzed.

FRAP acquisition settings

For Fig 8B-C and E-G and Fig EV5B, axons were imaged using a PerkinElmer Spinning Disk UltraVIEW ERS, Olympus IX81 inverted confocal microscope, 60X UPLSAPO objectives (NA 1.3), equipped with Hamamatsu C11440-22CU camera. Axons were photobleached with a 488 nm laser with the following settings: "60" for PK cycles; "1" for PK step size; "8000ms" for PK spot period; "2" for PK spot cycles; "Small" for PK spot size; "None" for PK attenuation. For Fig 8D, the labeled axons were visualized with an inverted TILL Photonics iMIC2, using a UPLSAPO 60x/1.2 water-immersion objective and an AVT Stingray F145B.30fps as detector. mRFP and Venus were visualized using an oligochrome Xenon arc lamp epifluorescence. Axons were photobleached with a 488 nm-laser using the following settings: dwell time (ms/µm^2) "1"; scan line "optimum"; line overlapping "41 %"; ROI loop count "1";

experiment loop count "10". Images for both mRFP and Venus were acquired before photobleaching, immediately after photobleaching, and then each minute for 10 minutes. Each image was captured with a Z-stack of 0.5 μm and an imaging depth of 2-3 μm. 100μM cyclohexamide (Sigma) was incubated 30 min before imaging, while Sema3A (R&D System) was added to the cultures immediately after photobleaching.

For *in vivo* FRAP (Fig 8E) electroporated embryos were raised until stage 40/41 and prepared for live imaging as previously reported (Wong *et al*, 2017). In particular, embryos were anaesthetized with 0.3mg/mL MS222 (Sigma) in 1x MMR, placed in a sylgard dish and secured with a custom made pin on their left side part. The part of the brain, controlateral to the electroporated eye, was exposed by removing the epidermis and the skin layers. The electroporated eye was removed in order to avoid trafficking from the soma to the RGC axonal compartment. Embryos were washed in 0.1mg/mL MS222 (Sigma) in 1x MMR once and mounted on an oxygenated chamber, obtained by superimposed two Gene Frame (ThermoFisher) on Nunc Permanox slides (ThermoFisher)filled with 0.1mg/mL MS222 (Sigma) in 1x MMR. Each image was captured with a Z-stack of 0.7 μm and an imaging depth of 7 μm.

Proximity ligation assay (PLA)

Stage 37/38 eyes were dissected and cultured for 24h. In some cases, the cultures were transfected either with co-MO 2μM or MOs-3p 2μM. Explants were then manually removed and isolated axons were co-stimulated for 10 min with 2ng/μL puromycin dihydrochloride (Sigma) and, 200ng/mL Sema3A (R&D System) or PBS 1x then fixed. Transfection was performed before the manual removal of the explants in order to preserve axonal health. Axons were washed 3 x 5 min in PBS 1X and then permeabilized with 0.1% Triton X-100 in PBS 1X for 10 minutes, rinsed once and washed 3x 5 min in 0.01% Triton X-100 in PBS 1X. The cultures were incubated with Duolink® Blocking Solution (Sigma) for 1 hour at 37°C and then incubated overnight at 4°C with primary antibodies diluted in Duolink® Antibody Diluent (Sigma). Rabbit anti-TUBB3 (T2200, 1:1000, Sigma) and anti-Puromycin (MABE343, 1:500, Merck Millipore) were used. Cultures were then washed with Duolink® In Situ Wash Buffer A (Sigma) 3 x 5min and incubated for 1 hour at 37°C with Duolink® In Situ PLA®PLUS and MINUS probes

(Sigma), diluted both 1:40 in Duolink® Antibody Diluent (Sigma). PLA was then carried out according to manufacturer's instructions aside from washes which were performed 3 times instead of 2. Controls were performed on two other independent experiments.

Imaging was performed using inverted Leica DMi8 epifluorescence microscope equipped with a sCMOS monochromatic camera (AndorZyla 4.2 Megapixel) and with a HC PL Apo CS2 63x/1.4 immersion oil objective. The acquisition mode was set to 12-bit grayscale and "high well capacity". Exposure time was kept consistently low for all channels (100ms). Healthy (e.g. non-collapsed growth cone in PBS control) and Sema3A-responsive growth cones were selected for analysis from single axons to avoid experimental bias. Unhealthy axons were not considered suitable for analysis.

Proximity ligation assay (PLA) analysis

Growth cones were all analyzed at the same image magnification (200%). The area of the growth cone was traced manually in the phase acquisition and then the number of puncta present in the fluorescence acquisition was counted manually. The puncta were identified by shifting the dynamic range so that every peak of fluorescence could be clearly distinguished. Only single axons were analyzed.

Plasmids

A plasmid list can be found in Table EV4. The 3'UTRs of TUBB3 chL (Xelaev18022595m.g), APP chL (Xelaev18011533m.g), and THBS1 chL (Xelaev18042667m.g) were cloned into the pCS2 Venus plasmid between monomeric Venus coding sequence and polyA signal. RNA from stage 37/38 eyes was reverse transcribed with SuperScript III (ThermoFisher) using 50 µM Oligo(dT) primers (Euroclone), and PCR reaction with Q5 High-Fidelity DNA Polymerase (NEB) was performed following the manufacturer's instructions. The mutated fragment after gel extraction and purification (QIAquick Gel Extraction Kit, Qiagen) were joint through overlapping-extension PCR (OE-PCR). Two out of the three MREs in THBS1 3' UTR were mutated through OE-PCR, while a third site, close to the 5' part of the amplicon was

inserted by Q5 mutagenesis kit (NEB) following manufacturer's instructions (primer sequences can be found in Table EV4).

Inserts were ligated into the plasmid using T4 DNA Ligase (NEB) and high-efficiency competent E.coli cells (#C2987, NEB) were transformed following manufacturer's instructions. The coding sequence of CD63 (Xelaev16074748m.g) was synthesized by GenScript and cloned into pCS2-eGFP plasmid, upstream of the GFP fluorescence protein, after digestion with ClaI-EcoRI enzymes (NEB), using T4 DNA Ligase (NEB) and clone into E.coli competent cells.

The coding sequence for Lamp1 chL (Xelaev18013051m.g) was synthesized and subcloned by GenScript in the pCS2-eGFP plasmids using Bsu15I-NcoI restriction enzymes, upstream of the GFP fluorescence protein. The DNA sequence of modified pre-miR-181a-1 without the loop was synthesized (see Table EV4 for sequence) and subcloned by GenScript in pUC57 vector with a T7 promoter for in vitro transcription.

Pre-miR synthesis and labelling

The DNA template for the synthesis of pre-miR-181a-1 was obtained by elongation of two oligos (Table EV4) complementary over 23bp (100µM each), while the synthesis of modified pre-miR-181a-1 without loop was obtained by PCR amplification of a pUC57-pre-miR-181a-1-noloop plasmid (GenScript). The primers were annealed, elongated at 12°C using 25U T4 DNA polymerase (NEB) and the obtained DNA fragment was purified with NucleoSpin PCR Clean-up kit (Macherey-Nagel).

The pre-miR-181a-1 and modified pre-miR-181a-1 without loop *in vitro* synthesis was performed using T7 MEGAshortscript™ kit (Ambion) from 1 µg purified DNA and following manufacturer's instructions, including DNase TURBO digestion step to remove the template following transcription. 5 µg of the product was labeled with cy3 or cy5 using Nucleic Acid Labeling Kit (Mirus) following the manufacturer's instructions.

Molecular beacon

Labeled molecular beacon probes with sequence 5'- CA**UUG C{C}UUUA{G}AUAC CAA**UG -3' was synthesized by Eurogentec (Belgium). The sequence in bold indicates the portion of the probe's loop that is complementary to the pre-miR-181a-1 sequence. We used the *in silico* RNA and DNA folding prediction algorithm DinaMelt to design adequate thermodynamic characteristics (Markham & Zuker, 2005). We selected the GC content of the stem according to the recommended 30-60% (Bratu *et al*, 2011), so that the melting temperature Tm of our MB was adapted to our working temperature (i.e. Tm 20-30°C higher than 20°C), ensuring that, when unbound, it is in a closed conformation, stable and does not fluoresce whilst spontaneously anneals to its target. We designed a backbone composed of 2'-O-methyl ribose and included 2 centrally placed LNA nucleotides (bracket), as they improve avoiding nuclease digestion stability but also hybridization efficiency and probe specificity (Kierzek *et al*, 2005; Majlessi *et al*, 1998). MB was designed to maximize signal-to-noise ratio by choosing an appropriate fluorophore, cy3, and associated quencher "black hole quencher 2" (BHQ2) and a strong 5-nt stem with an adequate melting temperature (Tm) to ensure that the probe does not fluoresce when unbound or when used at 20°C, our working temperature (Baker *et al*, 2013; Tyagi & Alsmadi, 2004). Cy3 quantum yield (Φ) is sensitive to high temperature (Φ decreases by 70% at 65°C compared to RT).

The reverse complement of the MB was blasted (www.xenbase.org) to check for possible off-targets in *Xenopus laevis*. The blast tool "blastn-DNA query to DNA database" was used, selecting as database "Xenopus Laevis J-strain 9.1 Genome" and as E value cut off 10. Blast against the whole genome was selected to investigate also possible off-targets on ncRNAs and the E value cut off was set at 10 to detect even the less probable off-targets (Table EV2). MB sequence or part of its sequence was complementary to additional 8 genomic loci but no corresponding reads were detected in axons by RNA-seq analysis. Therefore, MB does not match any known *Xenopus laevis* RNA sequence within the axon besides pre-miR-181a-1 (Table EV2). Tests *in vitro* indicated that the MB is stable in presence of DNAse I or total eye lysate (data not shown). Our MB design had suitable thermodynamic

characteristics of: low fluorescence at low temperature and a melting temperature (Tm) of 58°C, appropriate for our working temperature of 20°C.

Image processing

Images were adjusted for brightness and contrast. Gaussian blur convolution operation was applied using ImageJ software to prepare representative figures (Fig 1N, Fig2B, Fig3B,E,I, Fig 4C,E,G, Appendix Fig S1K,L, Appendix Fig S2B,E and Appendix Fig S3B,E,F).

BIBLIOGRAPHY

Baker MB, Bao G & Searles CD (2013) The Use of Molecular Beacons to Detect and Quantify MicroRNA. In *Methods in molecular biology (Clifton, N.J.)* pp 279–287.

Baudet M-L, Zivraj KH, Abreu-Goodger C, Muldal A, Armisen J, Blenkiron C, Goldstein LD, Miska EA & Holt CE (2012) miR-124 acts through CoREST to control onset of Sema3A sensitivity in navigating retinal growth cones. *Nature Neuroscience* **15:** 29–38

Bellon A, Iyer A, Bridi S, Lee FCY, Ovando-Vázquez C, Corradi E, Longhi S, Roccuzzo M, Strohbuecker S, Naik S, Sarkies P, Miska E, Abreu-Goodger C, Holt CE & Baudet M-L (2017) miR-182 Regulates Slit2-Mediated Axon Guidance by Modulating the Local Translation of a Specific mRNA. *Cell reports* **18:** 1171–1186

Bolger AM, Lohse M & Usadel B (2014) Trimmomatic: a flexible trimmer for Illumina sequence data. *Bioinformatics* **30:** 2114–2120

Bratu DP, Catrina IE & Marras SAE (2011) Tiny molecular beacons for in vivo mRNA detection. *Methods in molecular biology (Clifton, N.J.)* **714:** 141–57

Kierzek E, Ciesielska A, Pasternak K, Mathews DH, Turner DH & Kierzek R (2005) The influence of locked nucleic acid residues on the thermodynamic properties of 2'-O-methyl RNA/RNA heteroduplexes. *Nucleic Acids Res* **33:** 5082–5093

Li H, Handsaker B, Wysoker A, Fennell T, Ruan J, Homer N, Marth G, Abecasis G, Durbin R & 1000 Genome Project Data Processing Subgroup (2009) The Sequence Alignment/Map format and SAMtools. *Bioinformatics* **25:** 2078–2079

Liao Y, Smyth GK & Shi W (2014) featureCounts: an efficient general purpose program for assigning sequence reads to genomic features. *Bioinformatics* **30:** 923–930

Majlessi M, Nelson NC & Becker MM (1998) Advantages of 2'-O-methyl oligoribonucleotide probes for detecting RNA targets. *Nucleic acids research* **26:** 2224–9

Markham NR & Zuker M (2005) DINAMelt web server for nucleic acid melting prediction. *Nucleic Acids Research* **33:** W577–W581

Quast C, Pruesse E, Yilmaz P, Gerken J, Schweer T, Yarza P, Peplies J & Glöckner FO (2012) The SILVA ribosomal RNA gene database project: improved data processing and web-based tools. *Nucleic Acids Research* **41:** D590–D596

Robinson MD, McCarthy DJ & Smyth GK (2010) edgeR: a Bioconductor package for differential expression analysis of digital gene expression data. *Bioinformatics* **26:** 139–140

Ruthardt N, Lamb DC & Bräuchle C (2011) Single-particle Tracking as a Quantitative Microscopy-based Approach to Unravel Cell Entry Mechanisms of Viruses and Pharmaceutical Nanoparticles. *Molecular Therapy* **19:** 1199–1211

Simon B, Sandhu M & Myhr KL (2010) Live FISH: Imaging mRNA in living neurons. *Journal of Neuroscience Research* **88:** 55–63

Søe MJ, Møller T, Dufva M & Holmstrøm K (2011) A Sensitive Alternative for MicroRNA In Situ Hybridizations Using Probes of 2'-O-Methyl RNA + LNA. *Journal of Histochemistry & Cytochemistry* **59:** 661–672

Tinevez J-Y, Perry N, Schindelin J, Hoopes GM, Reynolds GD, Laplantine E, Bednarek SY, Shorte SL & Eliceiri KW (2017) TrackMate: An open and extensible platform for single-particle tracking. *Methods* **115:** 80–90

Turner-Bridger B, Jakobs M, Muresan L, Wong HH-W, Franze K, Harris WA & Holt CE (2018) Single-molecule analysis of endogenous β-actin mRNA trafficking reveals a mechanism for compartmentalized mRNA localization in axons. *Proceedings of the National Academy of Sciences of the United States of America* **115:** E9697–E9706

Tyagi S & Alsmadi O (2004) Imaging native beta-actin mRNA in motile fibroblasts. *Biophysical journal* **87:** 4153–62

Wong HH-W, Lin JQ, Ströhl F, Roque CG, Cioni J-M, Cagnetta R, Turner-Bridger B, Laine RF, Harris WA, Kaminski CF & Holt CE (2017) RNA Docking and Local Translation Regulate Site-Specific Axon Remodeling In Vivo. *Neuron* **95:** 852-868.e8